J|A|C|S
ARTICLES
Published on Web 09/23/2006

Characterization of Self-Assembled Monolayers of Fullerene Derivatives on Gold Surfaces: Implications for Device Evaluations

Yasuhiro Shirai, Long Cheng, Bo Chen, and James M. Tour*

Contribution from the Department of Chemistry, Smalley Institute for Nanoscale Science and Technology, Rice University, MS-222, 6100 Main Street, Houston, Texas 77005

Received May 17, 2006; E-mail: tour@rice.edu

Abstract: The widely employed approach to self-assembly of fullerene derivatives on gold can be complicated due to multilayer formations and head-to-tail assemblies resulting from the strong fullerene−fullerene and fullerene−gold interactions. These anomalies were not examined in detail in previous studies on fullerene self-assembled monolayers (SAMs) but were clearly detected in the present work using surface characterization techniques including ellipsometry, cyclic voltammetry (CV), and X-ray photoelectron spectroscopy (XPS). This is the first time that SAMs prepared from fullerene derivatives of thiols/thiol esters/disulfides have been analyzed in detail, and the complications due to multilayer formations and head-to-tail assemblies were revealed. Specifically, we designed and synthesized several fullerene derivatives based on thiols, thiol acetates, and disulfides to address the characterization requirements, and these are described and delineated. These studies specifically address the need to properly characterize and control fullerene−thiol assemblies on gold before evaluating subsequent device performances.

Introduction

Advances in molecular science continue to push forward the miniaturization of devices and the innovation of new molecule-based functional systems.[1] Of particular importance for our group are the fields with potential applications of fullerenes and fullerene derivatives. Since the discovery of fullerenes,[2] due to their unusual structure and optical and electrical properties, there has been a tremendous amount of research aimed at developing new fullerene-based materials with novel useful applications.[3] The combination of self-assembled monolayer (SAM) formation,[4] an important aspect in the field of molecular electronics,[5] with the advantageous properties of fullerene derivatives could lead to advances in this field.[3,6] In fact, many groups have worked to construct SAMs of fullerenes or fullerene derivatives on a variety of substrates including conductive surfaces such as gold[7,8] and other nonconductive, semiconductive, or transparent conductive surfaces including indium−tin oxide (ITO).[9] Among them, studies on gold surfaces are particularly extensive due to the well-defined organosulfur adsorption chemistry on Au surfaces.[4] Thiols, thiol esters, or disulfides are known to be absorbed onto a gold surface to form a SAM simply by exposing

(1) (a) Timp, G. L. *Nanotechnology*; AIP Press/Springer: New York, 1999. (b) *Nanoelectronics and Information Technology: Advanced Electronic Materials and Novel Devices Information Technology*; Waser, R., Ed.; Wiley-VCH: Weinheim, Germany, 2003. (c) Joachim, C.; Gimzewski, J. K.; Aviram, A. *Nature* **2000**, *408*, 541−548. (d) Forrest, S. R. *Nature* **2004**, *428*, 911−918.
(2) Kroto, H. W.; Heath, J. R.; O'Brien, S. C.; Curl, R. F.; Smalley, R. E. *Nature* **1985**, *318*, 162−163.
(3) (a) Prato, M. *Top. Curr. Chem.* **1999**, *199*, 173−187. (b) Konishi, T.; Ikeda, A.; Shinkai, S. *Tetrahedron* **2005**, *61*, 4881−4899.
(4) Love, J. C.; Estroff, L. A.; Kriebel, J. K.; Nuzzo, R. G.; Whitesides, G. M. *Chem. Rev.* **2005**, *105*, 1103−1169 and references therein.
(5) Tour, J. M. *Molecular Electronics: Commercial Insights, Chemistry, Devices, Architecture and Programming*; World Scientific: River Edge, NJ, 2003.
(6) (a) Mirkin, C. A.; Caldwell, W. B. *Tetrahedron* **1996**, *52*, 5113−5130. (b) Zeng, C.; Wang, H.; Wang, B.; Yang, J.; Hou, J. G. *Appl. Phys. Lett.* **2000**, *77*, 3595−3597.
(7) (a) Caldwell, W. B.; Chen, K.; Mirkin, C. A.; Babinec, S. J. *Langmuir* **1993**, *9*, 1945−1947. (b) Arias, F.; Godínez, L. A.; Wilson, S. R.; Kaifer, A. E.; Echegoyen, L. *J. Am. Chem. Soc.* **1996**, *118*, 6086−6087. (c) Domínguez, O.; Echegoyen, L.; Cunha, F.; Tao, N. *Langmuir* **1998**, *14*, 821−824. (d) Sahoo, R. R.; Patnaik A. *J. Colloid Interface Sci.* **2003**, *268*, 43−49. (e) Pan, G.-B.; Liu, J.-M.; Zhang, H.-M.; Wan, L.-J.; Zheng, Q.-Y.; Bai, C.-L. *Angew. Chem., Int. Ed.* **2003**, *42*, 2747−2751. (f) Patnaik, A.; Setoyama, H.; Ueno, N. *J. Chem. Phys.* **2004**, *120*, 6214−6221. (g) Yoshimoto, S.; Saito, A.; Tsutsumi, E.; D'Souza, F.; Ito, O.; Itaya, K. *Langmuir* **2004**, *20*, 11046−11052. (h) Bonifazi, D.; Spillmann, H.; Kiebele, A.; de Wild, M.; Seiler, P.; Cheng, F.; Güntherodt, H.-J.; Jung, T.; Diederich, F. *Angew. Chem., Int. Ed.* **2004**, *42*, 4759−2763. (i) Zhang, S.; Palkar, A.; Fragoso, A.; Prados, P.; de Mendoza, J.; Echegoyen, L. *Chem. Mater.* **2005**, *17*, 2063−2068. (j) Zhang, S.; Echegoyen, L. *J. Org. Chem.* **2005**, *70*, 9874−9881.
(8) (a) Shi, X.; Caldwell, W. B.; Chen, K.; Mirkin, C. A. *J. Am. Chem. Soc.* **1994**, *116*, 11598−11599. (b) Kim, S.; Park, S.-K.; Park, C.; Jeon, C., II. *J. Vac. Sci. Technol., B* **1996**, *14*, 1318−1321. (c) Imahori, H.; Ozawa, S.; Ushida, K.; Takahashi, M.; Azuma, T.; Ajavakom, A.; Akiyama, T.; Hasegawa, M.; Taniguchi, S.; Okada, T.; Sakata, Y. *Bull. Chem. Soc. Jpn.* **1999**, *72*, 485−502. (d) Imahori, H.; Azuma, T.; Ozawa, S.; Yamada, H.; Ushida, K.; Ajavakom, A.; Norieda, H.; Sakata, Y. *Chem. Commun.* **1999**, 557−558. (e) Shon, Y.-S.; Kelly, K. F.; Halas, N. J.; Lee, T. R. *Langmuir* **1999**, *15*, 5329−5332. (f) Kelly, K. F.; Shon, Y.-S.; Lee, T. R.; Halas, N. J. *J. Phys. Chem. B* **1999**, *103*, 8639−8642. (g) Fibbioli, M.; Bandyopadhyay, K.; Liu, S.-G.; Echegoyen, L.; Enger, O.; Diederich, F.; Bühlmann, P.; Pretsch, E. *Chem. Commun.* **2000**, 339−340. (h) Lee, S.; Shon, Y.-S.; Lee, T. R.; Perry, S. S. *Thin Solid Films* **2000**, *358*, 152−158. (i) Liu, S.-G.; Martineau, C.; Raimundo, J.-M.; Roncali, J.; Echegoyen, L. *Chem. Commun.* **2001**, 913−914. (j) Zhang, S.; Dong, D.; Gan, L.; Liu, Z.; Huang, C. *New J. Chem.* **2001**, *25*, 606−610. (k) Du, C.; Xu, B.; Li, Y.; Wang, C.; Wang, S.; Shi, Z.; Fang, H.; Xiao, S.; Zhu, D. *New J. Chem.* **2001**, *25*, 1191−1194. (l) Hoang, V. T.; Rogers, L. M.; D'Souza, F. *Electrochem. Commun.* **2002**, *4*, 50−53. (m) Imai, H.; Iwata, N.; Yamamoto, H. *Nanotechnology* **2002**, *13*, 768−770. (n) Yamada, H.; Imahori, H.; Fukuzumi, S. *J. Mater. Chem.* **2002**, *12*, 2034−2040. (o) Kim, K.-S.; Kang, M.-S.; Ma, H.; Jen, A. K.-Y. *Chem. Mater.* **2004**, *16*, 5058−5062. (p) Kang, S. H.; Ma, H.; Kang, M.-S.; Kim, K.-S.; Jen, A. K.-Y.; Zareie, M. H.; Sarikaya, M. *Angew. Chem., Int. Ed.* **2004**, *43*, 1512−1516. (q) Gu, T.; Whitesell, J. K.; Fox, M. A. *J. Org. Chem.* **2004**, *69*, 4075−4080. (r) Grüter, L.; Cheng, F.; Heikkilä, T. T.; González, M. T.; Diederich, F.; Schönenberger, C.; Calame, M. *Nanotechnoloty* **2005**, *16*, 2143−2248. (s) Zhang, S.; Echegoyen, L. *Tetrahedron* **2006**, *62*, 1947−1954.

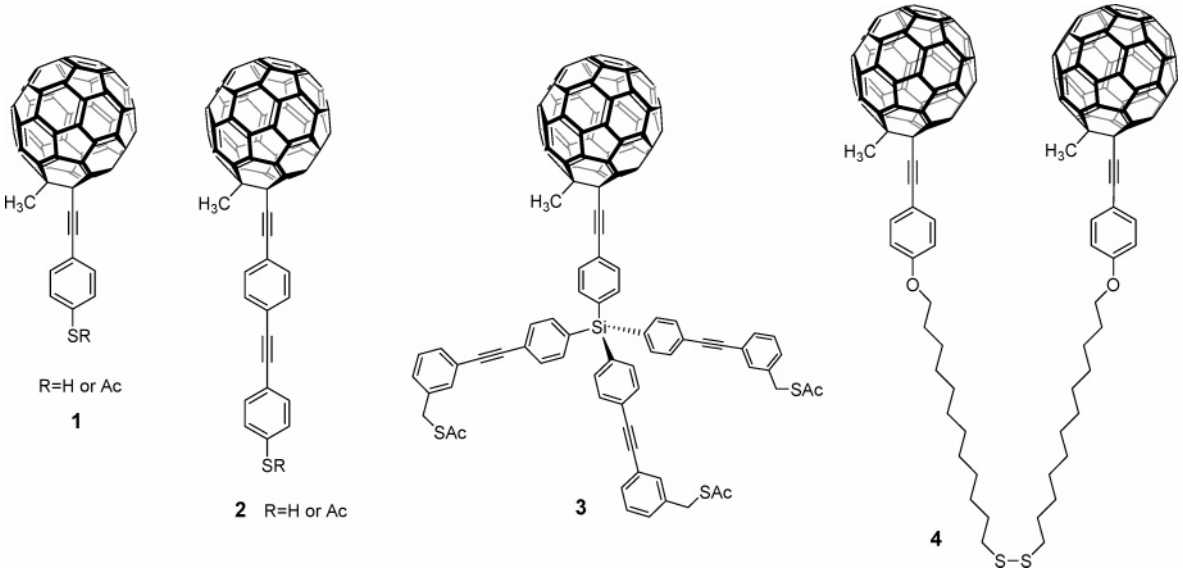

Figure 1. Fullerene−oligo(phenylene ethynylene) (OPE) hybrids **1** and **2**, fullerene tripod **3**, and fullerene disulfide **4** were used in this study.

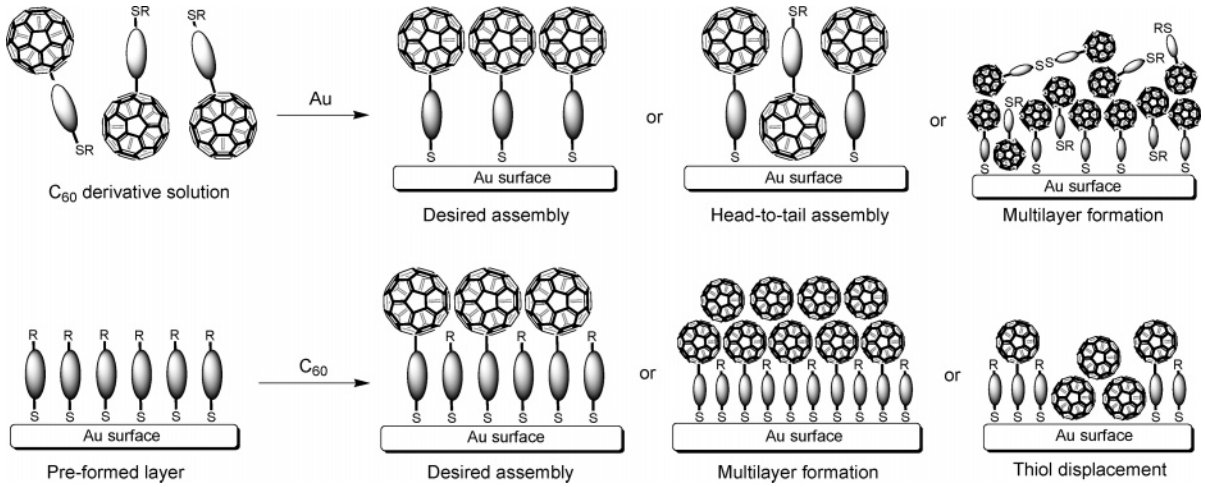

Figure 2. Two approaches to prepare fullerene SAMs, the direct method (top) and the indirect method (bottom), and possible anomalies introduced during SAM formation.

the gold surface to a solution of the molecule. In most instances, this simple view of SAM formation on gold has been assumed to be true for fullerene derivatives as well. However, we have found that this is not the case for the fullerene derivatives in our work (Figure 1) and is likely not the case for other fullerene derivatives that are similar to those shown in Figure 1. We report here anomalies associated with SAMs of these fullerene derivatives on gold using surface characterization techniques including ellipsometry, X-ray photoelectron spectroscopy (XPS), and cyclic voltammetry (CV). We also show that active control of the packing density of fullerene SAMs using the rigid molecular tripod[10] **3** is a promising (easy and reproducible) way to achieve highly electrochemically active fullerene SAMs.

There are two approaches to prepare SAMs of fullerene derivatives on gold (Figure 2). In the first approach, which we shall call the "direct" method, fullerene derivatives containing "alligator clips"[11] are synthesized so that they can bind to the

(9) (a) Chen, K.; Caldwell, W. B.; Mirkin, C. A. *J. Am. Chem. Soc*. **1993**, *115*, 1193−1194. (b) Chupa, J. A.; Xu, S.; Fischetti, R. F.; Strongin, R. M.; McCauley, J. P., Jr.; Smith, A. B., III; Blasie, J. K. *J. Am. Chem. Soc*. **1993**, *115*, 4383−4384. (c) Tsukruk, V. V.; Lander, L. M.; Brittain, W. J. *Langmuir* **1994**, *10*, 996−999. (d) Feng, W.; Miller, B. *Langmuir* **1999**, *15*, 3152−3156. (e) Kim, K.; Song, H.; Park, J. T.; Kwak, J. *Chem. Lett*. **2000**, 958−959. (f) Yamada, H.; Imahori, H.; Nishimura, Y.; Yamazaki, I.; Ahn, T. K.; Kim, S. K.; Kim, D.; Fukuzumi, S. *J. Am. Chem. Soc*. **2003**, *125*, 9129−9139. (g) Imahori, H.; Kimura, M.; Hosomizu, K.; Sato, T.; Ahn, T. K.; Kim, S. K.; Kim, D.; Nishimura, Y.; Yamazaki, I.; Araki, Y.; Ito, O.; Fukuzumi, S. *Chem.—Eur. J*. **2004**, *10*, 5111−5122. (h) Gulino, A.; Bazzano, S.; Condorelli, G. G.; Giuffrida, S.; Mineo, P.; Satriano, C.; Scamporrino, E.; Ventimiglia, G.; Vitalini, D.; Fragalà, I. *Chem. Mater*. **2005**, *17*, 1079−1084.

(10) For examples of tripod-shaped thiol derivatives, see: (a) Fox, M. A.; Whitesell, J. K.; McKerrow, A. J. *Langmuir* **1998**, *14*, 816−821. (b) Yao, Y.; Tour, J. M. *J. Org. Chem*. **1999**, *64*, 1968−1971. (c) Hu, J.; Mattern, D. L. *J. Org. Chem.* **2000**, *65*, 2277−2281. (d) Zhu, L.; Tang, H.; Harima, Y.; Yamashita, K.; Hirayama, D.; Aso, Y.; Otsubo, T. *Chem. Commun.* **2001**, 1830−1831. (e) Hirayama, D.; Takimiya, K.; Aso, Y.; Otsubo, T.; Hasobe, T.; Yamada, H.; Imahori, H.; Fukuzumi, S.; Sakata, Y. *J. Am. Chem. Soc*. **2002**, *124*, 532−533. (f) Zhu, L.; Tang, H.; Harima, Y.; Yamashita, K.; Aso, Y.; Otsubo, T. *J. Mater. Chem*. **2002**, *12*, 2250−2254. (g) Otsubo, T.; Aso, Y.; Takimiya, K. *J. Mater. Chem*. **2002**, *12*, 2565−2575. (h) Li, Q.; Rukavishnikov, A. V.; Petukhov, P. A.; Zaikova, T. O.; Keana, J. F. W. *Org. Lett*. **2002**, *4*, 3631−3634. (i) Jian, H.; Tour, J. M. *J. Org. Chem*. **2003**, *68*, 5091−5103. (j) Wei, L.; Padmaja, K.; Youngblood, W. J.; Lysenko, A. B.; Lindsey, J. S.; Bocian, D. F. *J. Org. Chem*. **2004**, *69*, 1461−1469. (k) Park, J.-S.; Nguyen Vo, A.; Barriet, D.; Shon, Y.-S.; Lee. T. R. *Langumuir* **2005**, *21*, 2902−2911. (l) Kitagawa, T.; Idomoto, Y.; Matsubara, H.; Hobara, D.; Kakiuchi, T.; Okazaki, T.; Komatsu, K. *J. Org. Chem*. **2006**, *71*, 1362−1369. (m) Yam, C. M.; Cho, J.; Cai, C. *Langmuir* **2003**, *19*, 6862−6868. (n) Moore, A. M.; Dameron, A. A.; Mantooth, B. A.; Smith, R. K.; Fuchs, D. J.; Ciszek, J. W.; Maya, F.; Yao, Y.; Tour, J. M.; Weiss, P. S. *J. Am. Chem. Soc.* **2006**, *18*, 1959−1967.

gold surfaces.[8] Alternatively, in an "indirect" method, a gold surface can be modified with an alligator clip-containing intermediate to which the fullerene can be attached in a second step.[7] Despite extensive literature on the preparation of SAMs of fullerene derivatives on gold surfaces, little or no attention has been paid to the strong interactions between fullerenes themselves, or between fullerenes and the gold surfaces, during the SAM formation except for the work by Kelly, et al.[8f] Because of the relatively strong adhesion of fullerenes onto gold surfaces (30−60 kcal/mol, vide infra),[12] which are similar to the Au−S bond strengths, and the tendency of fullerenes to form clusters,[13] one could imagine that fullerenes might form anomalous SAMs such as head-to-tail assemblies and multilayer formations (Figure 2). Furthermore, some thiol groups can be hampered from binding to the gold surface due to strong lateral fullerene−fullerene interactions; this is illustrated in the cartoon depicting several possible modes of multilayer formation via the direct SAM formation method (Figure 2). However, these aspects were not well addressed in previous studies on the self-assembly of fullerene-derivatized free or protected thiols. The indirect approach in Figure 2 could eliminate the formation of head-to-tail assemblies. However, multilayer formation can still occur if inappropriate solvents are chosen in the fullerene assembly. Moreover, the displacement of thiols by fullerenes must be considered. In some applications, a fullerene multilayer is actually desired and intentionally induced.[14] Nevertheless, the direct approach is more popular than the indirect one presumably due to the difficulties associated with carrying out chemical reactions on surfaces. If one could assume that the well-known simple chemistry of thiol-based SAM formation on gold is appropriate for fullerene derivatives, then the direct approach would be much simpler in terms of characterization. Using molecules shown in Figure 1 and surface characterization techniques including ellipsometry, XPS, and CV on electrode surfaces, here we show that this simple view is not appropriate for fullerene derivatives and the effects from the anomalies on the fullerene SAMs such as head-to-tail assembly and multilayer formation have to be considered in the design of fullerene-based functional devices.

Results and Discussion

Approaches to molecular electronics using OPE devices[15] have gained considerable attention since the successful demonstration of switching effects using this class of compounds.[16] To further advance the development of OPE devices for molecular electronics applications, we investigated fullerene−OPE hybrid devices such as **1** and **2** (Figure 1). These fullerene-derivatized OPEs with thiol and protected thiol alligator clips can be easily prepared using our in situ ethynylation method (Schemes 1−4).[17] This class of fullerene-derivatized OPEs is unique in that one can expect periconjugation[18] effects due to the close proximity between the fullerene and OPE π systems.

Scheme 1. Synthesis of the Fullerene−OPE Hybrids **1-SH** and **1-SAc**

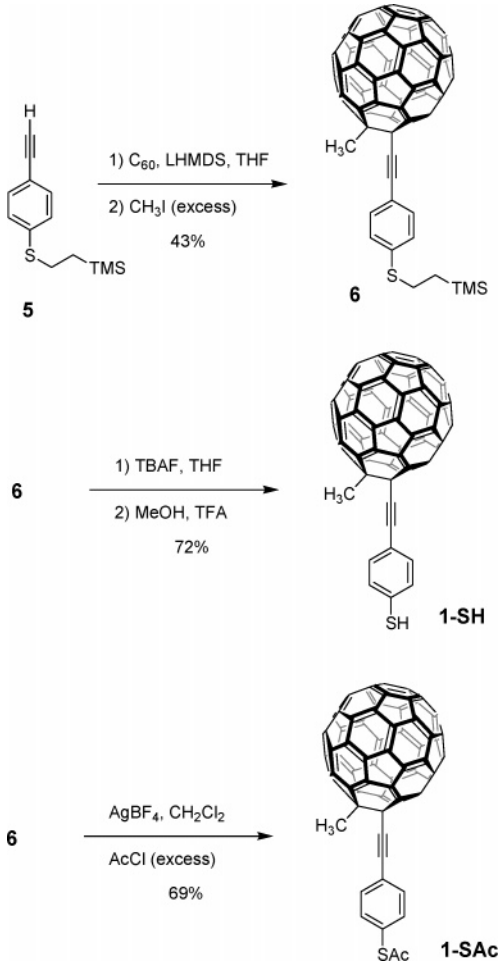

After synthesizing the fullerene−OPE molecules, they were then assembled onto gold surfaces using common assembly techniques (see the Experimental Section). However, the unusual results of the growth kinetics (Figure 3) of the fullerene−OPE hybrid **1** caught our attention.

Under all conditions except mixtures of 1,2-dichlorobenzene (ODCB), multilayer formation was evident even though the concentrations were kept to a minimum (less than 30 μM) to avoid aggregations of the fullerene derivatives during assembly periods. The ellipsometric thicknesses for **1** assembled from ODCB solutions were close to those predicted (1.8 nm). It is likely that **1** formed aggregates during assembly in the other solvents since the solubility of fullerene or fullerene derivatives in ODCB is generally quite high compared to that in the organic solvents toluene, CH_2Cl_2, and THF.[19] Our results demonstrate the importance of solvent choice for the assembly of fullerene

(11) Tour, J. M.; Jones, L., II; Pearson, D. L.; Lamba, J. S.; Burgin, T.; Whitesides, G. W.; Allara, D. L.; Parikh, A. N.; Atre, S. *J. Am. Chem. Soc.* **1995**, *117*, 9529−9534.
(12) (a) Chase, S. J.; Bacsa, W. S.; Mitch, M. G.; Pilione, L. J.; Lannin, J. S. *Phys. Rev. B* **1992**, *46*, 7873−7877. (b) Altman, E. I.; Colton, R. J. *Surf. Sci.* **1993**, *295*, 13−33. (c) Tzeng, C.-T.; Lo, W.-S.; Yuh, J.-Y.; Chu, R.-Y.; Tsuei, K.-D. *Phys. Rev. B* **2000**, *61*, 2263−2272. (d) Hunt, M. R. C.; Modesti, S.; Rudolf, P.; Palmer, R. E. *Phys. Rev. B* **1995**, *51*, 10039−10047.
(13) Patnaik, A.; Okudaira, K. K.; Kera, S.; Setoyama, H.; Mase, K.; Ueno, N. *J. Chem. Phys.* **2005**, *122*, 154703.
(14) Kamat, V. P.; Barazzouk, S.; Thomas, K. G.; Hotchandani, S. *J. Phys. Chem. B* **2000**, *104*, 4014−4017.
(15) (a) Tour, J. M.; Rawlett, A. M.; Kozaki, M.; Yao, Y.; Jagessar, R. C.; Dirk, S. M.; Price, D. W.; Reed, M. A.; Zhou, C.-W.; Chen, J.; Wang, W.; Campbell, I. *Chem.−Eur. J.* **2001**, *7*, 5118−5134. (b) James, D. K.; Tour, J. M. *Aldrichimica Acta* **2006**, *39*, 47−56. (c) James, D. K.; Tour, J. M. *Top. Curr. Chem.* **2005**, *257*, 33−62.
(16) Chen, J.; Reed, M. A.; Rawlett, A. M.; Tour, J. M. *Science* **1999**, *286*, 1550−1552.
(17) Shirai, Y.; Zhao, Y.; Cheng, L.; Tour, J. M. *Org. Lett.* **2004**, *6*, 2129−2132.
(18) (a) Zhao, Y.; Shirai, Y.; Slepkov, A. D.; Cheng, L.; Alemany, L. B.; Sasaki, T.; Hegmann, F. A.; Tour, J. M. *Chem.−Eur. J.* **2005**, *11*, 3643−3658. (b) Hamasaki, R.; Ito, M.; Lamrani, M.; Mitsuishi, M.; Miyashita, T.; Yamamoto, Y. *J. Mater. Chem.* **2003**, *13*, 21−26 and references therein.

Scheme 2. Synthesis of the Fullerene−OPE Hybrids **2-SH** and **2-SAc**[a]

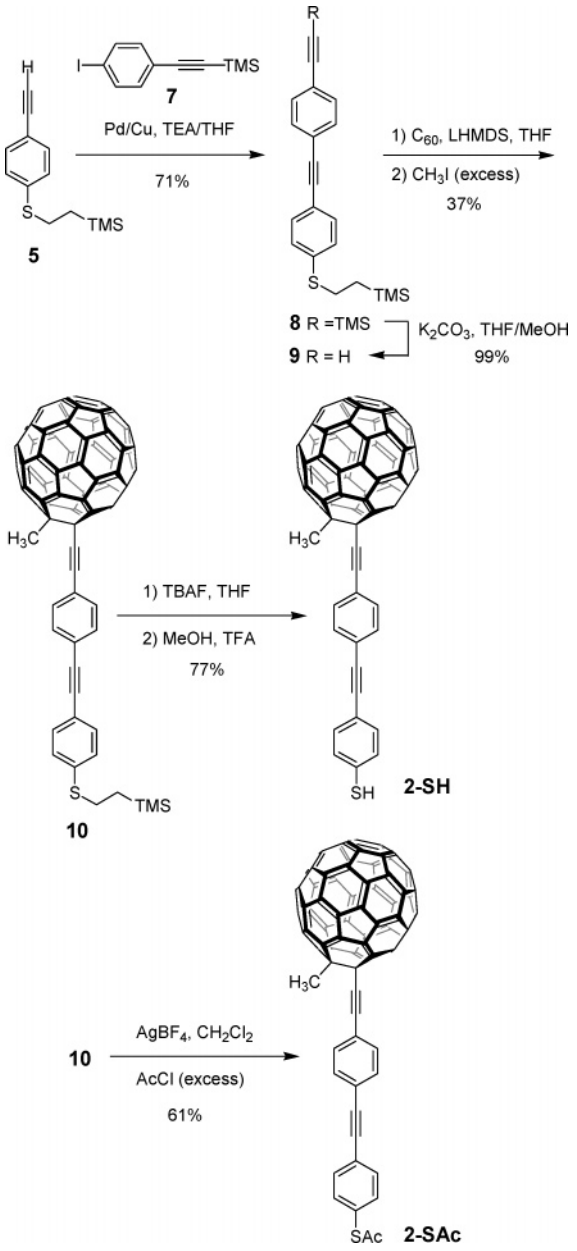

[a] Reagents: Pd/Cu = $PdCl_2(PPh_3)_2$, CuI.

derivatives and also the importance of ellipsometry measurements to detect multilayer formation. It is surprising that, to our knowledge, this is the first example of the use of ellipsometry to address multilayer formation in the assembly of fullerene-derivatized thiol or thiol esters.[20] For compounds with good solubility in common organic solvents, such as **3** and **4**, one may be able to assume that there is no significant multilayer formation during assembly. Otherwise, it is necessary to check the SAM thicknesses or deposited amounts with appropriate techniques such as ellipsometry or quartz crystal microbalance (QCM) measurements.[7a]

The film thickness of all compounds determined by ellipsometry is summarized in Table 1. All experiments were performed in the mixture of ODCB/EtOH (4:1); the EtOH was added to suppress oxidation of sulfur atoms (see the XPS results for the effect of EtOH in ODCB solution). In most cases, ellipsometric thicknesses reasonably correspond to the expected film thicknesses considering that ellipsometry is only accurate to within ±2 Å.[21] When free thiol compounds **1-SH** or **2-SH** were assembled in air, the resulting films were consistently thicker than those assembled in a nitrogen atmosphere. It is likely that the aryl thiols formed disulfide bonds under ambient conditions. Our previous studies on multifullerene derivatives, including difullerenes, determined that they are quite insoluble even in organic solvents such as CS_2 and ODCB.[17,18a,22] Thus, the disulfides generated in situ during the assembly will deposit on the surfaces. Therefore, we do not recommend the use of unprotected arylthiol derivatives for fullerene derivative SAM formation because mitigating disulfide formation is difficult. Figure 4 shows the assembly of fullerene derivatives **1**−**4** in ODCB/EtOH (4:1) solvent mixtures. Aryl thioacetates were deprotected in situ under acidic conditions[23] to avoid disulfide formation. In all cases, excessive multilayer formations are reasonably suppressed.

CV Characterization of SAMs. Because fullerene is electrochemically active, the resultant fullerene−OPE SAMs can be further characterized using CV. Figure 5 shows voltammograms from SAMs of **1-SAc** (acid deprotected) and **4** on Au electrode surfaces. The surface electrochemistry of the fullerene-derivatized Au electrode exhibited broad featureless spectra for these compounds, regardless of the different deposition time, concentration, solvent, and deprotection conditions. In the first few scans for the SAM of **1-SAc**, there were sometimes several features, as shown in Figure 5A, which are likely the redox signals from fullerenes. However, these features immediately disappeared in succeeding scans, and eventually the voltammograms became broad and featureless. The initial features observed upon CV were probably caused by fullerene derivatives loosely associated with the electrode surfaces by means of weak interactions such as physisorption. In many cases, shown in Figure 5B as representative voltammograms, we observed featureless broad voltammograms even in the initial scans. We observed similar behaviors for all SAMs prepared from **1**, **2**, and **4**.

Mirkin et al. and others previously reported the coverage-dependent electrochemical behavior of fullerene SAMs.[6a,7a,8q] It was shown that a tightly packed SAM could inhibit charge-compensating ion transport within the SAM film, leading to an electrochemical behavior that is drastically different from the one for the same redox-active molecule in solution.[24] Because our fullerene−OPEs **1**, **2**, and **4** can also form dense monolayers

(19) The solubility of fullerene in CH_2Cl_2, toluene, and ODCB is 0.3, 2.2, and 27 mg/mL, respectively: (a) Taylor, R. *The chemistry of Fullerenes*; World Scientific: River Edge, NJ, 1995. (b) Scrivens, W. A.; Tour, J. M. *J. Chem. Soc., Chem. Commun.* **1993**, 1207−1209.

(20) Previously, SAMs from fullerene-derivatized disulfides were checked using ellipsometry. However, the examples are similar to **4** in this work, structurally quite soluble in organic solutions, and unlikely to form multilayers; see: refs 8e and 8h.

(21) Azzam, R. M. A.; Bashara, N. M. *Ellipsometty and Polarized Light*; North-Holland: New York, 1987.

(22) Shirai, Y.; Osgood, A. J.; Zhao, Y.; Yao, Y.; Saudan, L.; Yang, H.; Yu-Hung, C.; Alemany, L. B.; Sasaki, T.; Morin, J.-F.; Guerrero, J. M.; Kelly, K. F.; Tour, J. M. *J. Am. Chem. Soc.* **2006**, *128*, 4854−4864.

(23) Cai, L.; Yao, Y.; Yang, J.; Price, D. W.; Tour, J. M. *Chem. Mater.* **2002**, *14*, 2905−2909.

(24) (a) Rowe, G. K.; Creager, S. E. *Langmuir* **1991**, *7*, 2307−2312. (b) Smith, C. P.; White, H. S. *Anal. Chem.* **1992**, *64*, 2398−2405. (c) Caldwell, W. B.; Campbell, D. J.; Chen, K.; Herr, B. R.; Mirkin, C. A.; Malik, A.; Durbin, M. K.; Dutta P.; Huang. K. G. *J. Am. Chem. Soc.* **1995**, *117*, 6071−6082.

Scheme 3. Synthesis of the Fullerene Tripod **3**[a]

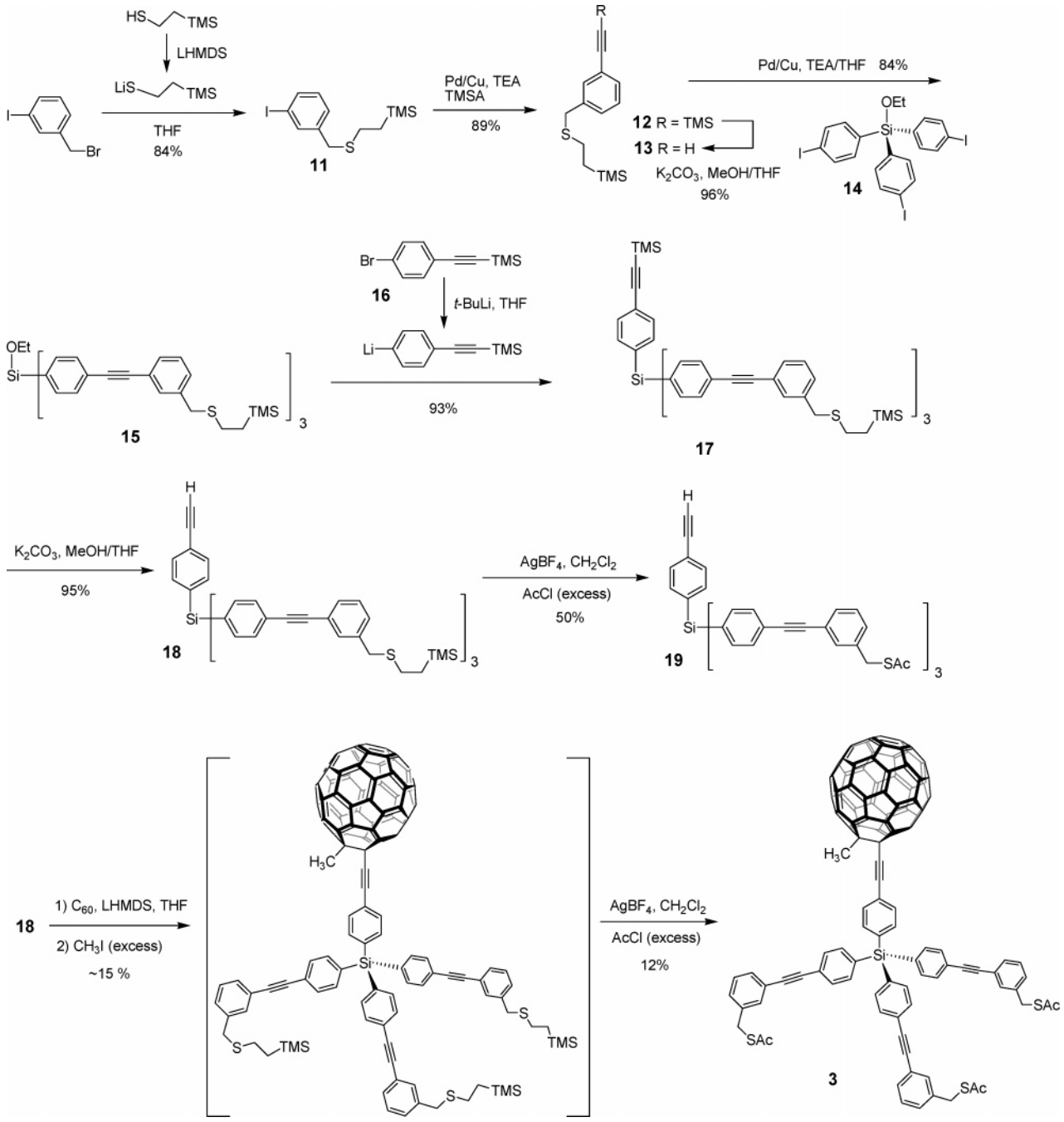

[a] Reagents: Pd/Cu = $PdCl_2(PPh_3)_2$, CuI.

due to interactions between the neighboring fullerenes, an effect similar to that reported by Mirkin et al. is probably causing the broad featureless voltammograms. Our attempts to obtain better-resolved electrochemical signals from less-than-monolayer-covered self-assemblies failed even though this strategy was previously reported to permit the ion transport effects.[8a] With our molecules, it was difficult to reproduce such partial coverage in a reliable manner. Controlling the spacing between the fullerenes by codeposition of inert compounds such as simple alkanethiols and arylthiols was also unsuccessful. This result actually parallels previous studies. When adsorbates can strongly interact with each other, it is difficult to avoid phase segregation within the mixed SAMs.[10m] To address this issue with a unique molecular design, we synthesized the fullerene tripod hybrid **3** that is designed to isolate the fullerene core from neighboring molecules using bulky tripod legs (Figure 6), allowing easy diffusion of charge-compensating ions within a SAM film.[10] The two well-resolved reversible redox waves, with reductions at −0.63 and about −0.99 V versus Ag/AgCl in Figure 7, indicate that this tripod strategy is in fact effective. As with other surface-confined fullerene species,[7−9] it was difficult to obtain a stable and reversible third redox wave that is observable in the solution state CV (see the Supporting Information for the solution state CV of fullerene and related compounds). For both of the redox signals, peak currents increase linearly with the scan rate (0.1−1.0 V/s) (Figure 7B), and the peak-to-peak separations are small ($\Delta E = 29.5 \pm 3.5$ mV) and independent of scan rates, indicating a typical behavior of surface-confined

Scheme 4. Synthesis of the Fullerene Disulfide **4**[a]

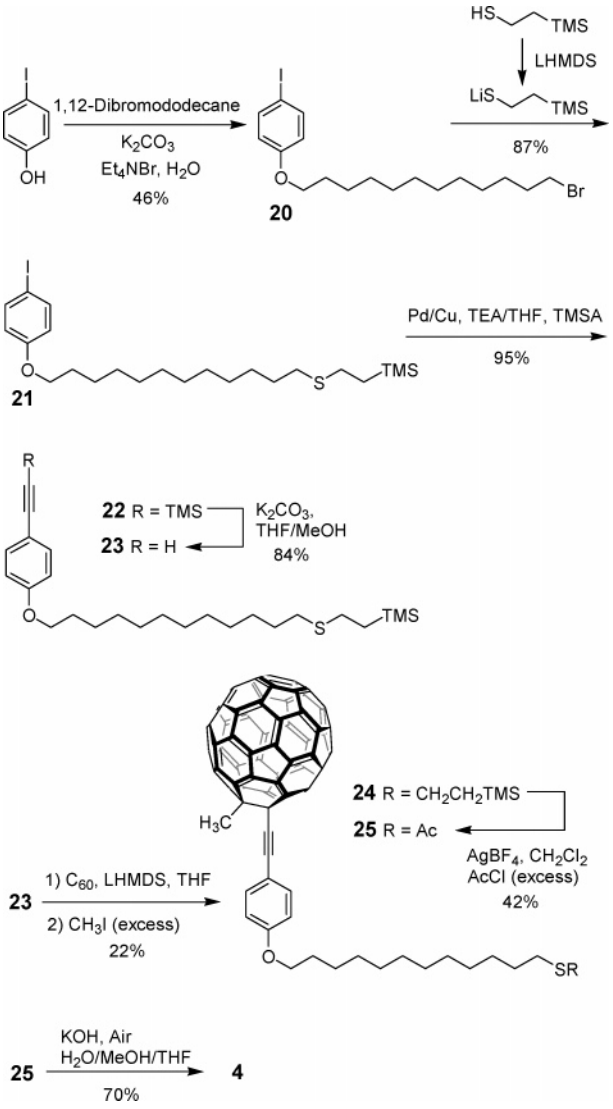

[a] Reagents: Pd/Cu = $PdCl_2(PPh_3)_2$, CuI.

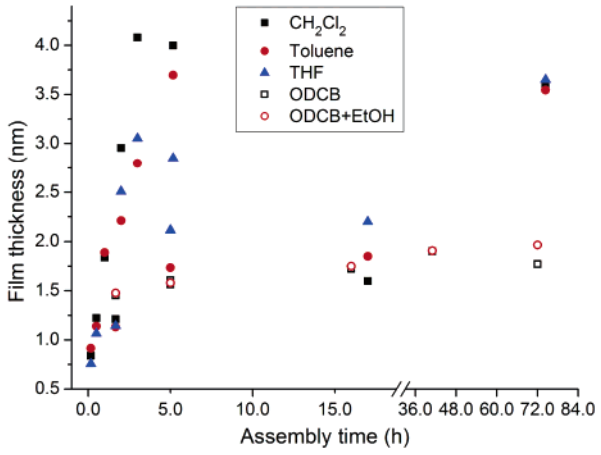

Figure 3. Growth kinetics of C_{60}−OPE hybrid **1** assembled on Au under different solvent conditions. The film thickness was determined by ellipsometry. Monolayer assembly would be reached at 1.8 nm. Data points with thicknesses >4.0 nm were not included in this chart.

electroactive species. With these well-behaved electrochemical responses and assuming all molecules on an Au electrode are electrochemically active, we estimated the footprint of **3** (nm^2/

Table 1. Assembly of the Fullerene Derivatives in a Solvent Mixture of ODCB[a]

compd	assembly condition[b]	time (h)	thickness (nm) exptl[c]	thickness (nm) calcd[d]
1-SH	N_2	24	1.7	1.8
1-SH	−	24	1.9	1.8
1-SAc	acid	24	1.7	1.8
2-SH	N_2	24	2.4	2.6
2-SH	−	24	2.7	2.6
2-SAc	acid	24	2.3	2.6
3	−	24	2.3	2.6
4	−	24	3.4	3.4

[a] Solvent mixture of ODCB/EtOH (4:1). [b] Acid: in ambient conditions and a catalytic amount of H_2SO_4 added in a capped container. −: in ambient conditions without acid in a capped container. N_2: assembly done in a nitrogen glovebox without acid. [c] The value measured by ellipsometry with an error of ±0.2 nm. [d] Distance between the gold atom and the top carbon atom in the fullerene cage. A linear Au−S−C bond angle with a 2.36 Å Au−S bond was assumed.

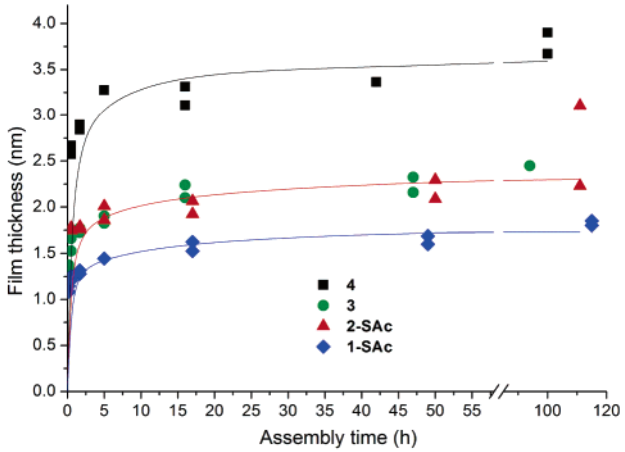

Figure 4. Growth kinetics of a series of fullerene derivatives assembled on Au in ODCB/EtOH (4:1) solvent mixtures. Film thickness was determined by ellipsometry. Compounds **1-SAc** and **2-SAc** were deprotected in situ using the acid deprotection method, while **3** and **4** were assembled without acid deprotection. All experiments were done under ambient conditions in a capped vessel, and the results from two separate experiments are shown for each compound.

molecule) using the Randles−Sevcik equation for a Nernstian reaction at the adsorbate monolayer (eq 1) or the integration of the area under the reduction waves,[25]

$$\mathrm{ip} = (9.39 \times 10^5) n^2 v A \Gamma \qquad (1)$$

where ip is the peak current in A, n is number of electrons, v is the scan rate in V/s, A is the electrode surface area in cm^2, and Γ is the coverage in mol/cm^2. For **3**, where $n = 1$, from a linear relationship between the scan rate v and the peak current ip and the predetermined electrode surface area A, Γ was estimated to be $3.8 \pm 0.1 \times 10^{-11}$ (mol/cm^2), and therefore the footprint of **3** is 4.4 nm^2/molecule. The integration of the area under the reduction waves also gave the coverage Γ in the same range ($2.8 \sim 5.0 \times 10^{-11}$ mol/cm^2). Figure 6 schematically compares this value to the size of molecule on a surface. For simplicity, in Figure 6 it has been assumed that the molecules in the SAM bind to the surface using all three of their thiolate ligands. However, the actual SAM is probably composed of a

(25) (a) Finklea, H. O. In *Electroanalytical Chemistry*; Bard, A. J., Rubinstein, I., Eds.; Marcel Dekker: New York, 1996; Vol. 19, pp 109−335. (b) Bard, A. J.; Faulkner, L. R. *Electrochemical Methods: Fundamentals and Applications*; John Wiley & Sons: New York, 2000.

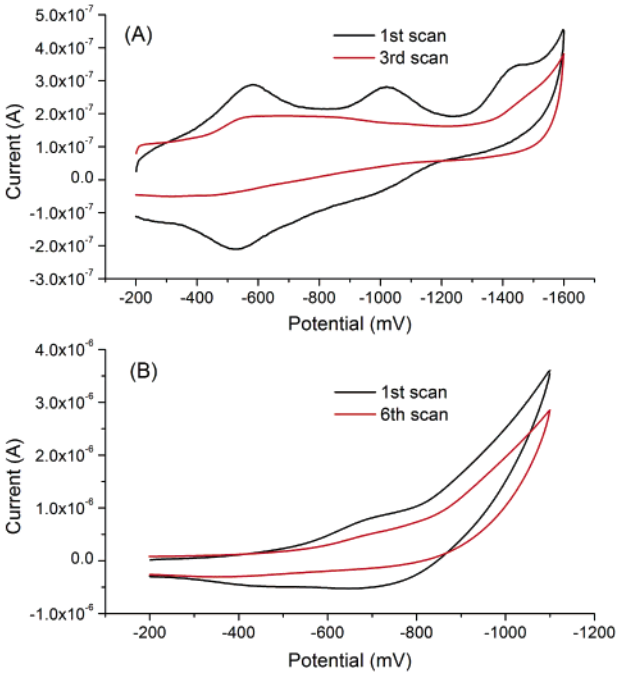

Figure 5. Cyclic voltammograms of SAMs of (A) **1-SAc** on a Au disk working electrode and (B) **4** on a Au bead working electrode in 0.1 M $TBAPF_6$ in ODCB/MeCN (4:1) at room temperature. **1-SAc** and **4** were assembled in ODCB/EtOH (4:1) with and without acid deprotection, respectively. The counter electrode was a Pt wire, and the reference electrode was Ag/AgCl. Scan rates were 100 mV/s.

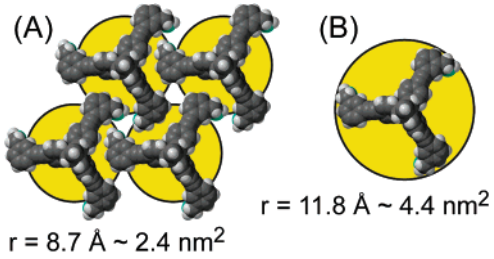

Figure 6. Schematics for the density of the tripod molecules **3** on the surface. It is assumed in this picture that all three thiolates bind to the surface. The fullerene moiety was not shown in the space-filling models for clarity. The small and large yellow circles are equivalent to an area of 2.4 and 4.4 nm^2, respectively, showing the area/molecule at (A) estimated minimum size, ~2.4 nm^2/molecule, and (B) estimated molecular footprint from CV results, ~4.4 nm^2/molecule.

mixture of several different conformations because **3** can bind to the surface using one, two, or three of its thiolate ligands; this, in combination with various conformations arising from fullerene−Au bonding, would lead to a loosely packed SAM.[10k,m,n] In comparison to the simulated crystalline packing of tripod **3** in Figure 6A, ($r \approx 8.7$ Å), the isolation (spacing) of fullerenes in the tripod SAM is increased according to our CV results ($r \approx 12$ Å, Figure 6B). The CV result confirms the noncrystalline, less-defined liquidlike loose packing of the tripod **3**. Our strategy of using a bulky tripod anchor group as a foundation of an electrochemically active site may be useful in other applications.[10]

XPS Analysis of Fullerene SAMs. The SAMs prepared from the fullerene derivatives of thiols/thiol esters/disulfides were further characterized using XPS. As mentioned earlier, fullerenes tend to form strong bonds on gold surfaces. Experimental[12] and theoretical[26] work, where fullerenes were deposited on gold surfaces in ultrahigh vacuum (UHV), supported the conclusion

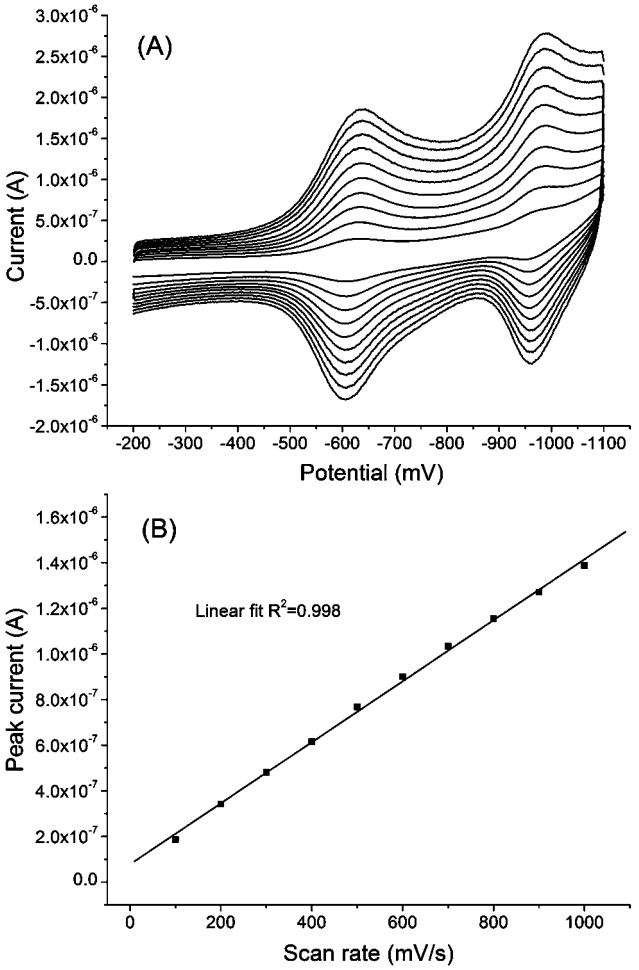

Figure 7. (A) Cyclic voltammograms of SAM of **3** on a Au bead working electrode in 0.1 M $TBAPF_6$ in ODCB/MeCN (4:1) at room temperature. The counter electrode was a Pt wire, and the reference electrode was Ag/AgCl. The scan rate was raised from 0.1 to 1.0 V/s with 0.1 V/s increments. (B) Peak currents at the first redox waves of part A as a function of scan rate.

that the strong adhesion between fullerenes and gold surfaces is either a charge-transfer interaction or covalent in nature with some ionic features. The adhesion energy was estimated to range from ~1.3 eV[26] to 2.2−2.6 eV[27] (from ~30 to 50−60 kcal/mol), which is comparable to ~50 kcal/mol for the Au−S bond.[4] In fact, the adhesion of fullerenes to gold surfaces allowed us to develop surface-rolling molecules, in which adhesion of the fullerenes to the gold surface was essential for the demonstration of rolling versus the more common sliding.[22,28] Furthermore, the fullerene/gold adhesion was not limited to the UHV-deposited fullerenes; studies in the solution phase also reported the adhesion of fullerenes onto gold surfaces.[29] The packing of fullerenes deposited from solutions corresponds to either a $(2\sqrt{3} \times 2\sqrt{3})R30$ arrangement with respect to the Au(111) lattice or an in-phase overlayer, which are essentially the same results as obtained on UHV-deposited fullerene overlayers on the same

(26) Wang, L.-L.; Cheng, H.-P. *Phys. Rev. B* **2004**, *69*, 165417−12.
(27) Guo, S.; Fogarty, D. P.; Nagel, P. M.; Kandel, S. A. *J. Phys. Chem. B* **2004**, *108*, 14074−14081 and references therein.
(28) Shirai, Y.; Osgood, A. J.; Zhao, Y.; Kelly, K. F.; Tour, J. M. *Nano Lett.* **2005**, *5*, 2330−2334.
(29) (a) Yoshimoto, S.; Narita, R.; Tsutsumi, E.; Matsumoto, M.; Itaya, K. *Langmuir* **2002**, *18*, 8518−8522. (b) Marchenko, A.; Cousty, J. *Surf. Sci.* **2002**, *513*, 233−237. (c) Uemura, S.; Samorí, P.; Kunitake, M.; Hirayama, C.; Rade, J. P. *J. Mater. Chem.* **2002**, *12*, 3366−3367.

substrates.[29b] These studies point to the possibility of the head-to-tail assembly of fullerene-derivatized organosulfurs on gold surfaces as shown in Figure 2. Surprisingly, however, the possibility of this head-to-tail assembly was not examined in detail in previous studies on the SAMs of thiols/thiol esters/disulfides of fullerene derivatives. In addition, to our knowledge, the XPS analysis on this class of compounds has not been reported.[30]

We addressed the possibility of the head-to-tail assembly of the fullerene derivatives along with other noticeable features using XPS because the difference in the chemical environments of the sulfur atoms that are bound or unbound to the gold surface is significant enough to be detected in a reliable manner.[31] Figure 8 shows representative detailed sulfur atom XPS spectra of the SAMs formed from **1**−**4**. There was a notable decrease in the ratio of unbound-to-bound sulfur atom signals, from 1.1 to 0.3, by doing the assembly in a nitrogen glovebox (Figure 8 and Table 2). This difference is likely the consequence of the decrease in the disulfide formation under nitrogen conditions, which is consistent with the ellipsometry data under the same conditions. A doublet centered at ∼169 eV was observed when the fullerene derivatives of unprotected thiols **1-SH** and **2-SH**, or disulfide **4**, were assembled using pure ODCB or a mixture of ODCB and EtOH solutions, whereas no such peak was detected when the thiol esters **1-SAc**, **2-SAc**, and **3** were assembled in the ODCB/EtOH solution. This high-energy sulfur signal is characteristic of highly oxidized sulfur atoms (+4 state, sulfonic acid).[32] Since our experimental conditions were consistent throughout all measurements, this feature was likely caused by either a difference in molecular structures or a difference in solvent conditions. We first examined the solvent conditions because the use of ODCB in SAM formation is rare.[33] A simple nonfullerene model compound, 4-bromobenzenethiol, was assembled in pure ODCB, EtOH, or mixtures of both,[34] and the resulting SAMs were examined using XPS (see the Supporting Information for the XPS spectra). Significant sulfur oxidation took place during assembly in pure ODCB solution, whereas no such signal was detected when pure EtOH was used. Because the use of ODCB is essential for the prevention of fullerene aggregation leading to the multilayer formation according to the ellipsometry analysis, we used a mixture of ODCB and EtOH, hoping that good solubility in ODCB paired with the reducing environment in EtOH would be mutually effective. We found this to be the case. Next, we looked at structural differences as a cause of sulfur oxidation and noticed that thiols **1-SH** and **2-SH** and disulfide **4** were readily oxidized, whereas sulfides (thiol esters **1-SAc**, **2-SAc**, and **3**) were less susceptible to the oxidation. This observation is actually parallel to the general trend in sulfur chemistry, in which thiols or disulfides are easily oxidized due to the weak S−H or S−S

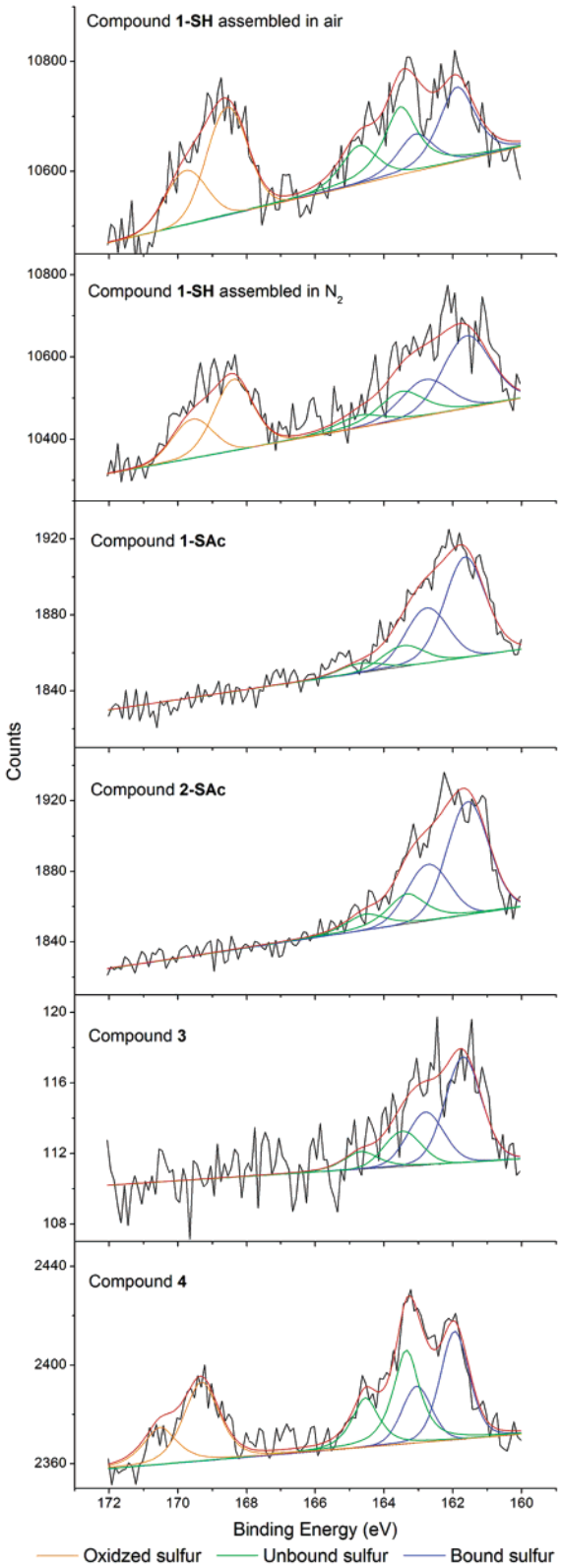

Figure 8. XPS S_{2p} spectra for **1-SH** assembled using ODCB in ambient (capped vessel) or in glovebox, **1-SAc** and **2-SAc** assembled in ODCB/EtOH (4:1) mixture using the in situ acid deprotection method in ambient conditions, and **3** and **4** assembled in ODCB/EtOH (4:1) mixture in ambient conditions. The broad peaks from 161 to 165 eV were fit using two S_{2p} doublets with 2:1 area ratios and splittings of 1.2 eV and one S_{2p} doublet with 2:1 area ratios and splittings of 1.2 eV for the peak at ∼169 eV. Each doublet is assigned to surface-bound, surface-unbound, and oxidized sulfur atoms.

(30) XPS analysis on fullerene-derivatized methyl sulfides was previously reported, see ref 8c. Methyl sulfides have a weak interaction with gold and are less frequently employed as an alligator clip.
(31) (a) Gastner, D. G.; Hinds, K.; Grainger, D. W. *Langmuir* **1996**, *12*, 5083−5086. (b) Yasseri, A. A.; Syomin, D.; Malinovskii, V. L.; Loewe, R. S.; Lindsey, J. S.; Zaera, F.; Bocian, D. F. *J. Am. Chem. Soc.* **2004**, *126*, 11944−11953.
(32) (a) Rieley, H.; Price, N. J.; Smith, T. L.; Yang, S. *J. Chem. Soc., Faraday Trans.* **1996**, *92*, 3629−3634. (b) Rieley, H.; Kendall, G. K.; Zemicael, F. W.; Smith, T. L.; Yang, S. *Langmuir* **1998**, *14*, 5147−5153.
(33) For an example of the use of ODCB as adsorbate solution, see ref 8i.
(34) We decided to use EtOH because it is the most widely used solvent for SAM formation and it is used to reduce Au surfaces after oxidative cleaning such as UV/ozone, thus producing a reducing environment. The mechanism for EtOH suppression of sulfur oxidation during assembly in ODCB is unknown at this point.

Table 2. Sulfur Atom Binding Energies and Atomic Ratios

	binding energy (eV)			estimated atomic ratio	
SAM	bound S $2p_{3/2}$	unbound S $2p_{3/2}$	oxidized S $2p_{3/2}$	unbound/ bound	oxidized/ bound
1-SH[a]	161.9	163.5	168.6	1.1	1.2
1-SH[b]	161.6	163.5	168.4	0.3	0.8
1-SAc[c]	161.6	163.5		0.2	0
2-SAc[c]	161.6	163.4		0.3	0
3[d]	161.6	163.5		0.4	0
4[d]	161.9	163.4	169.3	1.0	0.8

[a] SAM was prepared in ODCB in ambient (capped vessel) conditions. [b] SAM was prepared in ODCB in a glovebox. [c] In situ acid deprotection in a mixture of ODCB/EtOH (4:1) in ambient conditions. [d] Assembled in a mixture of ODCB/EtOH (4:1) in ambient conditions.

bond, respectively, and the oxidation will not stop until the sulfonic acid (+4 state) is produced.[35] A similar phenomenon was observed for the assembly of the acetyl-protected α,ω-dithiols,[36] in which no oxidation was detected. It is also possible that fullerene enhances sulfur oxidation because fullerene itself can be easily reduced (oxidizing surroundings). As a result, the mixture of ODCB and EtOH (4:1) can suppress the oxidation for the thiol esters **1-SAc**, **2-SAc**, and **3**. However, it was not effective enough for the more oxidation-susceptible thiols **1-SH** and **2-SH** and disulfide **4**.

For all SAMs of the fullerene-derivatized organosulfurs we tested, careful examination of the broad peaks from 161 to 165 eV suggests at least two doublets of S 2p signals (each with area ratios of 2:1 and splittings of 1.2 eV). It is likely that these doublets correspond to surface-bound (~161.7 eV for S $2p_{3/2}$) and surface-unbound (~163.5 eV for S $2p_{3/2}$) sulfur atoms.[31] The unbound thiol/thiol ester/disulfide S 2p signals may result from a number of possible species in the SAMs. The fullerene derivatives that are structurally poor in solubility, such as **1** and **2**, could be deposited on top of the fullerene monolayer, leading to multilayer formation. Alternatively, they could be trapped within the monolayer film without forming a sulfur−gold bond due to the strong lateral interactions between fullerenes. Either of these structures could contribute to the unbound S 2p signals. Even though the solubility of fullerene derivatives in the ODCB mixture is good, the possibility of deposition through precipitation cannot be ruled out because homocoupled difullerenes would be insoluble, leading to the disulfide S 2p signals. Another possible cause for the unbound S 2p signal is the head-to-tail assembly (Figure 2), in which the molecules assembled on Au via fullerene−Au surface adhesion, not the usual thiolate−Au bonding. This is especially true for highly soluble fullerene derivatives and thiol esters that will not form homocoupled difullerene species in situ. The well-solvated species are less likely to be trapped in the monolayer film or to be deposited on the surface of the SAM via precipitation; therefore, the unbound S 2p signals in these cases likely originate from the head-to-tail assembly. The disulfide **4** was designed to rule out the possibility of multilayer formation. Because it has a long alkyl chain, the molecule is quite soluble in the ODCB mixture and there is no in situ disulfide formation leading to precipitation and deposition onto surfaces. Furthermore, it is well established that alkanethiols with a polymethylene chain (number of the methylenes ≥10) form densely packed monolayers on gold surfaces.[8q,37] For these reasons, the disulfide **4** was supposed to form an ideal fullerene SAM on gold surfaces. However, the S 2p signals from the SAM of disulfide **4** (Figure 8) clearly indicate an ~1:1 mixture of (possibly alternating) head-to-tail assembled molecules. Ironically, even though the disulfide **4** was designed to minimize the unbound species, it gave the highest ratio in the unbound-to-bound S 2p signal.[38] This finding is important because fullerene derivatives of thiols/thiol esters/disulfides are believed to form unidirectionally assembled monolayers on gold surfaces. The fullerene SAMs were thus thought to be a useful and simple strategy to mimic the core of natural photosynthesis, in which the unidirectional multistep electron transfer occurs along well-arranged assemblies, leading to the generation of a charge-separated state across the membrane with quantum efficiency close to unity.[39] Because fullerene can be an excellent electron acceptor in a donor−acceptor electron-transfer system,[40] two-dimensional and unidirectional arrangement of such fullerene systems in the form of SAM on gold is attractive for the construction of high-efficiency artificial photosynthesis membranes.[41] However, our results indicate that a method similar to the indirect approach in Figure 2 may be preferred in order to attain a complete unidirectional assembly. It is difficult to rationalize why the disulfides **4** form SAMs with ~1:1 unbound-to-bound ratio. One possibility is that the densely packed SAM of **4** is more stable with the molecules alternatively arranged on the Au surface to maximize density or molecule-to-molecule interactions (Figure 9). In this case, the molecules, once trapped head-to-tail into a SAM, may not be able to flip over. The other fullerene derivatives **1** and **2** are unlikely to form such organized SAMs; thus, any head-to-tail packed molecules can flip over to maximize fullerene−fullerene interactions, thereby reducing the degree of the head-to-tail assembly. In all cases, the cross section mismatch between the fullerene head and the tether to the anchoring sulfur is evident (except for tripod **3**); this cross section mismatch could be a cause for the head-to-tail assembly.

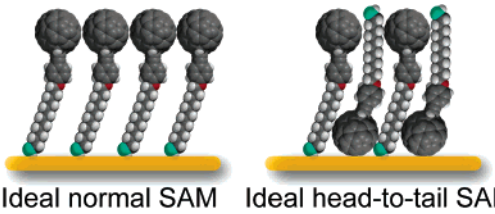

Figure 9. Schematics of ideal dense normal and head-to-tail SAMs of compound **4** on gold surfaces.

(35) Cremlyn, R. J. *An Introduction to Organosulfur Chemistry*; John Wiley & Sons: New York, 1996.
(36) Lau, K. H. A.; Huang, C.; Yakovlev, N.; Chen, Z. K.; O'Shea, S. J. *Langmuir* **2006**, *22*, 2968−2971.
(37) (a) Porter, M. D.; Bright, T. B.; Allara, D. L.; Chidsey, C. E. D. *J. Am. Chem. Soc.* **1987**, *109*, 3559−3568. (b) Imahori, H.; Azuma, T.; Ajavakom, A.; Norieda, H.; Yamada, H.; Sakata, Y. *J. Phys. Chem. B* **1999**, *103*, 7233−7237.
(38) The **1-SH** assembled under ambient conditions also had a high ratio of unbound-to-bound S 2p signal, but ellipsometrioc data indicated that multilayer formation, rather than head-to-tail assembly, was the main cause for the high ratio.
(39) (a) Ferreira, K. N.; Iverson, T. M.; Maghlaoui, K.; Barber, J.; Iwata, S. *Science* **2004**, *303*, 1831−1838. (b) Alstrum-Acevedo, J. H.; Brennaman, M. K.; Meyer, T. J. *Inorg. Chem.* **2005**, *44*, 6802−6827.
(40) (a) *Fullerenes: From Synthesis to Optoelectronic Properties*; Guldi, D. M., Martin, N., Eds.; Kluwer Academic Publishers: Dordrecht, The Netherlands, 2002. (b) Guldi, D. M.; Prato, M. *Acc. Chem. Res.* **2000**, *33*, 695−703.
(41) (a) Imahori, H.; Fukuzumi, S. *Adv. Funct. Mater.* **2004**, *14*, 525−536. (b) Imahori, H.; Yamada, H.; Nishimura, Y.; Yamazaki, I.; Sakata, Y. *J. Phys. Chem. B* **2000**, *104*, 2099−2108. (c) Imahori, H.; Yamada, H.; Ozawa, S.; Ushida, K.; Sakata, Y. *Chem. Commun.* **1999**, 1165−1166.

It is well established that trithiol species,[10] such as tripod **3**, often bind to Au surfaces with only one or two of the possible three S−Au bonds forming.[10k,m,n,31b] This could explain the slightly high unbound-to-bound ratio in tripod **3**, compared to the other monothiol derivatives **1** and **2**, because not all three thiols are bound to the Au surface in the SAM formed from **3**. This is especially true for the fullerene tripod **3** because the strong fullerene−Au interaction will compete with other S−Au interactions. Interestingly, a tripod molecule that does not contain fullerene, compound **19** (Scheme 3), also had a relatively high unbound-to-bound ratio (0.3) by XPS analysis (see the Supporting Information for the XPS spectrum of **19**).

Conclusions

In this article we have demonstrated that the seemingly simple and widely employed approach to self-assembly of fullerene derivatives on gold surfaces can be complicated due to multilayer formation and head-to-tail assemblies (Figure 2). These fullerene SAM anomalies have not been previously considered but were clearly detected using surface characterization techniques including ellipsometry, CV, and XPS. Ellipsometry analysis showed that the use of a combination of ODCB solvent and protected thiols was necessary in some cases due to the low solubility of fullerene derivatives and the insolubility of byproduct generated by in situ disulfide formation. However, the enhanced sulfur atom oxidation side effect of ODCB was detected by XPS analysis. The side effect could be suppressed by mixing EtOH with ODCB without drastically affecting the solubility of fullerene derivatives in the ODCB mixture. The XPS analysis of fullerene SAMs also showed a considerable amount of surface-unbound sulfur atoms along with surface-bound atoms. From this observation, and based on literature indicating the existence of strong fullerene−Au surface adhesion, we have proposed the head-to-tail assembly of fullerene SAMs (Figure 2), in which molecules are assembled on Au via fullerene−Au bonding, not the usual thiolate−Au bonding. The other possible cause of the surface-unbound sulfur atoms is the deposition of low-solubility fullerene derivatives on top of SAMs and trapping of the fullerene-containing molecules within the monolayer film, without forming a sulfur−gold bond, due to strong lateral fullerene−fullerene interactions. However, the assembly of disulfide **4**, in which the possibility of deposition of fullerene derivatives on top of SAMs is greatly reduced because of good solubility and an inability to generate insoluble disulfides in situ, further supports the head-to-tail assembly. Interestingly, disulfide **4** shows the highest ratio of unbound-to-bound S atoms even though it was designed to reduce the ratio. The cross section mismatch between the fullerene head and the tether to the anchoring sulfur can be a possible cause of the head-to-tail assembly. However, it would be challenging to eliminate the cross section mismatch because of the unusually large size of the fullerene moiety. Electrochemistry on these fullerene SAMs confirmed the effect of packing density on electrochemical responses that has been reported previously. Only the tripod **3**, that is designed to isolate the electroactive moiety in SAMs, showed ideal CV responses.

The application of fullerenes in a variety of molecule-based device applications appears promising due to their advantageous properties, and in fact, many studies on the SAM formation of fullerene derivatives on gold have been reported as one of the methods for the integration of fullerenes into device applications.[8] However, most of the previous reports assumed that fullerene derivatives follow the usual chemistry of SAMs on gold. Here we have shown that this assumption is inappropriate. The way that fullerenes are integrated into the device will seriously affect the overall device properties.

Experimental Section

Materials. The synthesis of fullerene derivatives **1**−**4** is reported in the Supporting Information. 4-Bromobenzenethiol was obtained from Lancaster and used as received. Anhydrous 1,2-dichlorobenzene (ODCB) and anhydrous THF were obtained from Sigma-Aldrich and degassed by bubbling nitrogen gas through them before use. Absolute ethanol (EtOH) was obtained from Pharmco and degassed as above. All other solvents used for self-assembly were freshly distilled over CaH_2. H_2SO_4 (96%) was obtained from Fisher and used as received. Si(100) wafers (p-doped, test grade) were obtained from Silicon Quest International.

Preparation of the Au Substrate. The silicon wafer was cleaned in a hot fresh Piranha (3:1 H_2SO_4/30% H_2O_2, v/v) solution for 10 min, rinsed with flowing distilled water, ethanol, and dried in flowing pure nitrogen gas. *Caution: Piranha reacts violently with organic compounds, and care should be taken while handling this mixture*. The Au films were deposited by thermal evaporation of 150−200 nm thick Au onto the silicon wafer with an ∼10 nm Cr adhesion layer at a rate of 1.2−1.3 Å/s at a base pressure of 1×10^{-6} torr. Before use, the Au substrates were cut into ∼1 cm^2 shards and cleaned by a UV/ozone cleaner (Boekel Industries, Inc., model 135500) for 10 min, followed by immersion in EtOH for at least 20 min.[42]

Chemical Assembly. The cleaned Au substrates were immersed into the adsorbate solutions at room temperature for a specified period. All the adsorbate solutions were freshly prepared in ambient or nitrogen atmosphere and kept in the dark during assembly. Typical concentrations were 15∼30 μM for **1** and **2** and 50∼100 μM for **3** and **4**. Precipitates that formed in the adsorbate solution of **1-SH** or **2-SH** were filtered though a plug of silica gel under nitrogen atmosphere before the immersion of the Au substrates. For in situ acid deprotection,[23] ∼50 μL of H_2SO_4 (96%) was added to about 20 mL of adsorbate solution, and the solution was incubated in a capped vessel for 30−60 min in order to deprotect the thiol moiety. After the assembly, the samples were removed from the solutions and quickly immersed in pure solvent of the same kind as in the adsorbate solution (for the mixtures of ODCB/EtOH, pure ODCB was used) to avoid precipitation of the fullerene derivatives, rinsed thoroughly with ODCB and EtOH, and finally blown dry with nitrogen.

Ellipsometry. Measurements of surface optical constants and molecular layer thicknesses were taken with a single-wavelength (632.8 nm laser) LSE Stokes ellipsometer (Gaertner Scientific). Measurements were carried out before and immediately after monolayer adsorption. The surface thickness was modeled as a single absorbing layer atop an infinitely thick substrate (fixed ns). The index of refraction was set at $n_f = 1.55$, $k_f = 0$. For growth kinetics measurements, each experiment consisted of ∼20 Au substrates, and at each specified period, three substrates were taken out from adsorption solutions and thicknesses were measured for each substrate and an average value was reported.

X-ray Photoelectron Spectroscopy (XPS) Measurements. A PHI Quantera SXM XPS/ESCA system at 5×10^{-9} torr was used to take photoelectron spectra. All samples were transferred to the UHV system within 20 min after the end of assembly to avoid excessive oxidation in air. Typical assembly time was 20−24 h. A 114.8 monochromatic Al X-ray source was applied for all measurements with an analytical spot size of 0.10 mm × 0.10 mm, a 45° takeoff angle, and a pass energy of 26.00 eV. High-resolution spectra of the S 2p region used a 45° takeoff angle and 13.00 eV pass energy. Unless noted, surface samples

(42) Ron, H.; Matlis, S.; Rubinstein, I. *Langmuir* **1998**, *14*, 1116−1121.

were referenced against the internal Au $4f_{7/2}$ line at 84.0 eV. Powder XPS photoelectron lines were referenced against the C 1s signal at 284.50 eV.

Electrochemical Measurements. CV experiments were performed on a BAS-CV 50W instrument. An aqueous Ag/AgCl reference electrode and a platinum wire as the counter electrode were used. All experiments were conducted under a N_2 atmosphere using mixture of ODCB/MeCN (4:1) containing 0.1 M Bu_4NPF_6 as the supporting electrolyte. The gold substrates for routine CV analysis were prepared by annealing the tip of a gold wire (99.999%, 0.5 mm diameter, Alfa Aesar) in a gas−oxygen flame. Subsequently, the hot Au bead was cooled in deionized water. The geometric area of the Au bead electrode touching electrolyte solution was typically 0.013−0.024 cm^2, which was used to determine the coverage Γ from the integration of reduction waves. For the determination of the surface coverage Γ using eq 1, PEEK-encased Au disk electrodes were used because of the well-defined surface area (typically $5.74-5.85 \times 10^{-3}$ cm^2), even though reduction waves obtained with this electrode were too small to integrate reliably. The geometric areas of the electrodes were obtained from the slope of a linear plot of the cathodic current versus (scan rate)$^{1/2}$ for the reversible reduction of the $Fe(CN)_6^{3-}$ in 0.1 M KCl, taking 0.76×10^{-5} cm^2/s as the diffusion coefficient and knowing the exact concentration from the mass (see the Supporting Information for details).

Acknowledgment. The Welch Foundation, DARPA/AFOSR, and the NSF Penn State MRSEC funded this work. We thank Drs. I. Chester of FAR Research Inc. and R. Awartani of Petra Research Inc. for providing the TMSA.

Supporting Information Available: Detailed syntheses of the new compounds, their NMR spectra, solution state CV of selected compounds, details of the CV calculations, and XPS spectra of 4-bromobenzenethiol and compound **19**. This material is available free of charge via the Internet at http://pubs.acs.org.

JA063451D